Ionization of boron, aluminum, gallium, and indium by electron impact

Yong-Ki Kim and Philip M. Stone
National Institute of Standards and Technology, Gaithersburg, Maryland 20899-8421
(Received 23 April 2001; published 4 October 2001)

Measurements of electron impact ionization of neutral Al, Ga, and In show large cross sections compared to other elements in the same rows of the periodic table. Semiempirical and classical calculations of direct ionization cross sections are all substantially smaller. Calculations by McGuire [Phys. Rev. A **26**, 125 (1982)] for aluminum that include excitations to autoionizing $3s3p^2$ doublet levels are 2.5 times higher than experiment at the peak. We report the direct ionization cross sections based on the binary-encounter-Bethe model of Kim and Rudd [Phys. Rev. A **50**, 3954 (1994)], which is an *ab initio* theory. We add the autoionization contribution using scaled plane-wave Born cross sections as recently developed by Kim [Phys. Rev. A **64**, 032713 (2001)] for excitations to the first set of autoionizing levels. Dirac-Fock wave functions are used for the atomic structure. Our results are in excellent agreement with experimental values and support substantial contributions from excitation-autoionization to the total ionization cross sections for these elements. We also compare the total ionization cross section of boron to available theories, though no experimental data are available.

DOI: 10.1103/PhysRevA.64.052707 PACS number(s): 34.80.Dp

I. INTRODUCTION

The latest measurement of electron-impact ionization of neutral aluminum shows a rather large cross section, especially compared with cross sections of other elements in the same row of the periodic table [1]. Existing theoretical calculations have not agreed well with these measurements. The semiempirical formula of Lotz [2] underestimates the peak value by more than 40%. The DM formalism of Margreiter *et al.* [3], which is a modification of Gryzinski's classical formula [4] with empirical parameters, shows better agreement at the peak but is too small at incident electron energies between the threshold and the peak. The plane-wave Born (PWB) calculation of McGuire [5] is much too large in the peak region and remains higher than experiment even at high energies. Mann [6] estimated peak cross sections using the mean square radius $\langle r^2 \rangle$ of the target orbitals calculated from Hartree-Fock wave functions. His peak cross section is too small by a factor of two.

The situation is similar for neutral Ga, the next element in the same column of the periodic table. Measurements by Shul *et al.* [7] and more recently by Patton *et al.* [8] agree with each other within 30%, but their cross sections are large compared to calculated values from the Lotz and the DM formulas. Indium is also similar. The cross section calculated from the DM formalism is smaller than the experimental results [1] by more than 30% between the threshold and the peak.

Several autoionizing levels—mainly $nsnp^2$ doublet levels—contribute significantly to the measured total ionization cross sections for these atoms. These levels lie several eV above the ionization limit, are easily excited by electron impact from the ground level, and decay almost entirely by autoionization. McGuire [5] has estimated the contribution of these autoionizing levels for Al using PWB cross sections for the primary electrons involved in both direct ionization and autoionization, but his cross sections are much too large, mostly because of the well-known limitations of the PWB approximation and the inadequate target wave functions he used.

Three decades ago, Peach [9] recognized the importance of excitation-autoionization of inner-shell electrons in her paper on the electron- and proton-impact ionization of neutral atoms. However, her emphasis was on the complete removal of the ns electron resulting in an excited ion in the $nsnp\ ^3P$ or ^1P level. Her results cannot be compared to the present paper because our cross sections are for the production of an ion in its ground level, $ns^2\ ^1S$.

We have used the binary-encounter-Bethe (BEB) model of Kim and Rudd [10] to calculate the direct ionization cross sections of B, Al, Ga, and In. To calculate the excitation-autoionization cross sections, we used the scaling methods recently developed by Kim [11] for plane-wave Born (PWB) cross sections. We used both uncorrelated and correlated Dirac-Fock wave functions for the target atoms. When applicable, we estimated and applied the branching ratios of these excited levels for autoionization versus fluorescent decay.

The BEB cross sections for the direct ionization and the scaled PWB cross sections for the excitation-autoionization are easy to generate in contrast to other computer-intensive theories such as the *R*-matrix method [12], the convergent close-coupling (CCC) method [13], the time-dependent close-coupling method [14], and the complex scaling method [15]. Some of these theoretical methods generate a complete set of cross sections, e.g., elastic, discrete excitation, and ionization including both angular distributions and integrated cross sections. The price for the complete information is the long time required even with the most powerful computers and, more importantly, limited applicability to targets with complex valence shell structures and heavy atoms.

On the other hand, the BEB method [10] generates direct ionization cross sections for any neutral atom (or molecule) using an analytic formula that requires only the data from ground-state wave functions, i.e., the orbital binding-energy B, orbital kinetic-energy $U=\langle p^2/2m \rangle$, and the orbital electron occupation number N for each orbital in the target. This method has been successfully applied to dozens of neutral molecules, H, He, and Xe [16–18].

In a recent article [11], it was shown that two simple

scaling methods could convert PWB excitation cross sections into reliable cross sections comparable to the most accurate theoretical or experimental data available for dipole-allowed excitations. These methods use PWB cross sections calculated from uncorrelated wave functions, and the scaling requires only the binding energy B of the electron being excited, the excitation energy E, and accurate dipole oscillator strength f, or the f value, if electron correlation strongly affects the f value. Again, because of its simplicity, these scaling methods can be used for dipole-allowed excitations of light and heavy atoms, such as H, He, Hg, and Tl [11].

The goal of the present paper is to demonstrate that the combination of the BEB model for direct ionization and the scaled PWB cross sections for excitation-autoionization produces total ionization cross sections of many atoms reliable in both magnitude—$\pm 15\%$ or better at the peak—and shape from the ionization threshold to a few keV in the incident electron energy. The theoretical methods we have used are summarized in Sec. II, and the calculated cross sections are compared to existing experimental and theoretical data in Sec. III. Our conclusions are presented in Sec. IV.

II. THEORY

The valence structure of the ground state of the atoms in the Group IIIB column headed by boron is given by $ns^2np\,^2P$. Excitation of the ns electron into np results in the $nsnp^2\,^4P$, ^2D, ^2S, and ^2P levels. The $ns-np$ excitation cross sections by electron impact are very large because they are dipole allowed and the initial and final states belong to the same shell with good overlap of the radial functions. In addition, the Group IIIB atoms have two ns electrons versus one np electron, thus making the autoionization contribution more conspicuous than the atoms in other columns of the periodic table.

Of the excited levels, the ^4P level does not contribute to autoionization because it is in the discrete spectrum for all atoms in the Group IIIB column. Some of the doublet levels, however, lie in the continuum of the direct ionization of the valence np electron. The continuum channels for the direct ionization of the np electron resulting from the dipole interaction has the ^2S and ^2D character. Hence, the $nsnp^2\,^2D$ and ^2S levels autoionize rapidly through the Auger process because the parity, spin, and orbital angular momenta match. On the other hand, the $nsnp^2\,^2P$ level is expected to be slow to autoionize because the parity does not match with the ^2P direct ionization channel. We checked the branching ratios of these autoionizing levels by comparing their autoionization and fluorescence rates—the Einstein A coefficients—calculated from Dirac-Fock wave functions as will be discussed later.

For boron, only the $2s2p^2\,^2P_{1/2}$ and $^2P_{3/2}$ levels are above the first ionization threshold while the other doublet levels are in the discrete spectrum. For aluminum, the $3s3p^2\,^2D$ level is not observed as it mixes strongly with the bound $3s^2nd\,^2D$ Rydberg series [19]. The $3s3p^2\,^2S_{1/2}$, $^2P_{1/2}$, and $^2P_{3/2}$ levels are in the continuum above the first ionization threshold and together they contribute nearly as much to Al ionization by autoionization as direct ionization. For Ga, In, and Tl, the $nsnp^2$ doublet levels are all in the continuum and contribute heavily to the total ionization cross section.

In addition to the autoionization of the $nsnp^2$ doublet levels, infinitely many autoionizing levels result from the excitation of the ns electrons to ml (e.g., $3d$, $4p$, etc. for Al). These levels together, however, contribute 5% at the most to the total ionization cross section, far less than the $nsnp^2$ doublet levels, as we shall demonstrate for aluminum. We have not included these minor autoionization channels for B, Ga, and In because, as stated earlier, our goal is to generate total ionization cross sections with an overall reliability of $\pm 15\%$ or better at the peak. In the remainder of this section, we briefly outline the theoretical models we have used to calculate cross sections for the direct ionization and autoionization.

A. Binary-encounter-Bethe model

The BEB model is a simplified version of the more detailed binary-encounter-dipole (BED) model developed by Kim and Rudd [10]. The BED model combines a modified form of the Mott cross section [20,21] with the Bethe theory [22,23]. The BED model starts with a singly differential cross section, or the energy distribution of secondary (=ejected) electrons, and requires the continuum oscillator strength, df/dE, where E is the excitation energy to the continuum, for each atomic orbital. The orbital cross sections are summed to get the energy-differential ionization cross section for the entire atom. To cover a wide range of the incident electron energy T, the BED model requires df/dE for each orbital to a few hundred eV in E.

The exact form of df/dE for H-like ions is known [24], while for other atoms, one can sometimes deduce df/dE from either theoretical or experimental photoionization cross sections. The BEB model uses a simple form for df/dE for each initial-state orbital when information on accurate df/dE is not available. The orbital ionization cross section in the BEB model is given by

$$\sigma_{\mathrm{BEB}}=\frac{S}{t+u+1}\left[\frac{\ln t}{2}\left(1-\frac{1}{t^2}\right)+1-\frac{1}{t}-\frac{\ln t}{t+1}\right], \qquad (1)$$

where $S=4\pi a_0^2 N(R/B)^2$, $t=T/B$, $u=U/B$, $a_0=0.529$ Å (Bohr radius), and $R=13.61$ eV (Rydberg energy). Although all input data needed in Eq. (1) can be obtained from the ground-state wave function, we use the experimental ionization energy for B for the valence electron because theoretical ionization energies rarely match the thresholds observed in ionization experiments.

The total ionization cross section is the sum of Eq. (1) over the orbitals of the target atom or molecule. Inner shell orbitals beyond the first few outer shells usually contribute little to the total ionization cross section because of their large binding energies.

We have obtained U and B for each orbital from Dirac-Fock wave functions [25]. A modification has been introduced into Eq. (1) to reduce $u+1$ in the denominator for atomic orbitals with $n\geqslant 3$, where n is the principal quantum

number. In earlier applications of the BEB model, Hwang *et al.* [26] found that the cross section is reduced too much by the $u+1$ term for these orbitals because the kinetic energy of valence orbitals with many radial nodes becomes high (e.g., $U=79.74$ eV, $B=12.56$ eV for Xe $5p$). The denominator $t+u+1$ on the right-hand side of Eq. (1) is therefore replaced by $t+(u+1)/n$ when $n\geqslant 3$. The reduction of $u+1$ is also consistent with the BE-scaling of the PWB cross sections discussed in Sec. II B.

B. BE scaling of plane-wave Born cross sections

A PWB cross section for electron-impact excitation has the form:

$$\sigma_{\mathrm{PWB}}=\frac{4\pi a_0^2 R}{T}F_{\mathrm{PWB}}(T), \tag{2}$$

where $F_{\mathrm{PWB}}(T)$ is the collision strength (different from the standard definition by a multiplicative constant).

The BE scaling replaces the T in the denominator on the right-hand side of Eq. (2) by $T+B+E$, i.e.,

$$\sigma_{\mathrm{BE}}=\sigma_{\mathrm{PWB}}T/(T+B+E), \tag{3}$$

where E is the excitation energy as defined earlier.

The replacement of T by $T+B+E$, or adding a constant to T, is similar in spirit to the Burgess scaling [21,27] used in Eq. (1), where T in the denominator on the right-hand side was replaced by $T+B+U$, which is $t+u+1$ in the threshold unit used in Eq. (1). Comparing the Burgess scaling in Eq. (1) to the scaling in Eq. (3) indicates that U plays the role of an average excitation energy for ionization. Note that the total ionization cross section described by Eq. (1) implies integration over the kinetic energy of an ionized electron, i.e., integration over energy transfers from the incident electron. Hence, U acts as a weighted average of the energy transfer from the incident electron to the ionized electron. This average energy transfer decreases as the principal quantum number of the bound electron increases because its binding energy decreases. This is consistent with the finding by Hwang *et al.* [26] that it is necessary to reduce $U+B$, or $u+1$ in the threshold unit, in Eq. (1) for valence electrons with high principal quantum numbers, as was described in Sec. II A.

Kim has shown many examples [11] in which the BE scaling by itself or in combination with the f scaling described below transformed PWB cross sections for dipole-allowed excitations into very reliable cross sections comparable to the CCC cross sections or highly accurate experiments. The BE scaling not only changes the magnitude but also the shape of the original PWB cross sections. The reason for the success of the BE scaling is not clear at present.

C. *f* scaling of plane-wave Born cross sections

Application of any collision theory to atoms with more than one bound electron must use approximate wave functions. The f value for a dipole-allowed transition is an atomic property sensitive to the accuracy of the wave functions used. Hence, it is natural to attempt to use f values to generate electron-impact cross sections, though the f value itself is used to determine photoabsorption cross sections. The Gaunt factor method [28] is an example, where known f values are used and the focus of the method is to find matching collision strengths.

In contrast, the f scaling proposed by Kim [11] retains the PWB collision strength $F_{\mathrm{PWB}}(T)$ defined in Eq. (2) without any change. Instead, the entire cross section is multiplied by the ratio of an accurate f value to the less accurate f value calculated from the single configuration wave functions used to generate the unscaled PWB cross sections. Since our goal is to generate ionization cross sections of modest accuracy, it is more efficient to take advantage of accurate f values if they are available from other sources, rather than divert our attention to the generation of highly accurate wave functions. The f scaling is defined by

$$\sigma_f=(f_{\mathrm{mc}}/f_{\mathrm{sc}})\sigma_{\mathrm{PWsc}}. \tag{4}$$

where σ_f is the f-scaled cross section; f_{mc} stands for an f value calculated from correlated, or multiconfiguration, wave functions; f_{sc} signifies an f value calculated from simple, or single configuration, wave functions; and σ_{PWsc} is the PWB cross section obtained from single-configuration wave functions from which f_{sc} was calculated. An accurate experimental f value could be used in place of f_{mc}.

The BE scaling and f scaling may be applied consecutively

$$\sigma_{\mathrm{BE}f}=\sigma_{\mathrm{BE}}\cdot(f_{mc}/f_{sc}). \tag{5}$$

Examples of successful applications of $\sigma_{\mathrm{BE}f}$ can be found in Ref. [11]. The BE and f scalings provide powerful means to convert PWB cross sections calculated from simple wave functions into highly accurate excitation cross sections with three atomic parameters B, E, and f value that in principle, can all be calculated from accurate wave functions. In reality, however, experimental values of the first ionization energy, most discrete excitation energies, and accurate f values for some transitions of neutral atoms are readily available [29].

III. RESULTS AND DISCUSSION

The present theoretical cross sections for the production of singly charged ions of B, Al, Ga, and In are shown in Figs. 1–4 with representative error limits for the quoted experimental data. The theoretical cross section curves for direct ionization and for direct plus autoionization in the figures clearly show that autoionization almost doubles ionization cross sections for these elements. The atomic parameters used in the present paper are listed in Table I. The resulting counting cross sections for direct and indirect ionization are listed in Tables II–V. We have included all bound electrons whose binding energies are less than 10 keV in the calculation of direct ionization cross sections using the BEB model.

Some older experimental data on Al, Ga, In and Tl by Shimon *et al.* [30], on Al by Golovach *et al.* [31], and on Ga and In by Vainshtein *et al.* [32] have not been included in our

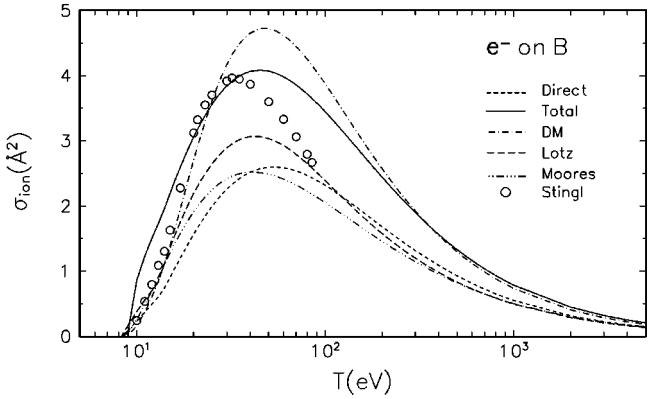

FIG. 1. Ionization cross section of B. All cross sections are for the production of singly charged ions only. Direct (short-dashed curve) = direct ionization, present paper; Total (solid curve) = direct ionization plus excitation-autoionization, present paper; DM (dot-dashed curve) = theory, DM formalism Ref. [3]; Lotz (long-dashed curve) = theory, Lotz formula [2]; Moores (dot-dot-dot-dashed curve) = theory, recommended by Moores [34]; Stingl (circles) = theory, Coulomb-Born approximation by Stingl [35].

comparison because these data show no resemblance to the shape of the cross sections shown in Figs. 2–4. The experimental and theoretical cross sections of Ga and In reported by Vainshtein *et al.* [32] are close to the direct ionization cross sections shown in Figs. 3 and 4. The paper by Vainshtein *et al.* also includes theoretical results based on the PW Born approximation and a method equivalent to the distorted-wave Born approximation. Their theoretical results, however, agree with their experimental data, which are significantly lower than the total ionization cross sections shown in Figs. 3 and 4.

In addition to the contributions from excitation-autoionization, the creation of inner-shell holes results in the

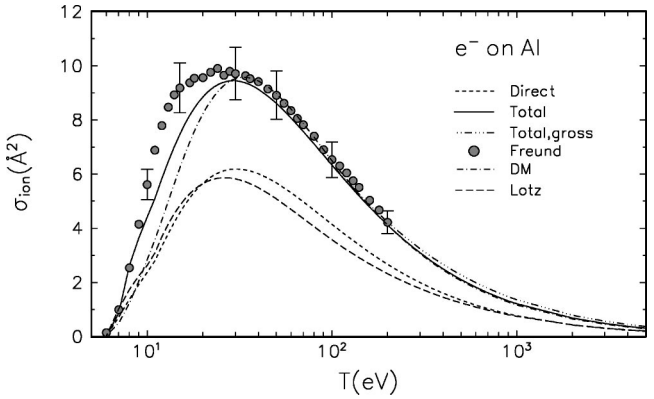

FIG. 2. Ionization cross section of Al. All cross sections are for the production of singly charged ions only, except for the total gross ionization cross section, Eq. (7). Direct (short-dashed curve) = direct ionization, present paper; Total (solid curve) = direct ionization plus excitation-autoionization, present paper; Total, gross (dot-dot-dot-dashed curve) = gross ionization, present paper; Freund (circles) = experiment by Freund *et al.* [1]; DM (dot-dashed curve) = theory, DM formalism Ref. [3]; Lotz (long-dashed curve) = theory, Lotz formula [2].

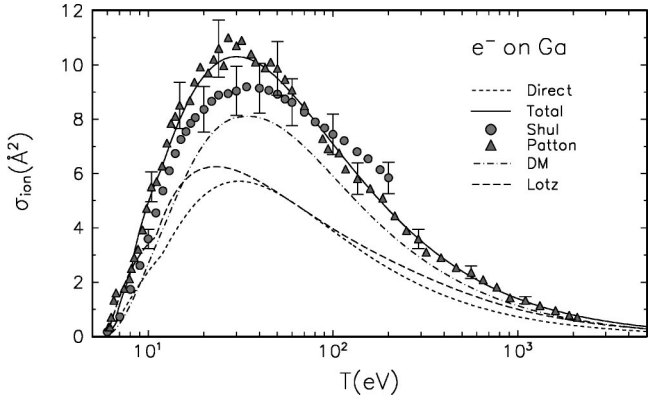

FIG. 3. Ionization cross section of Ga. All cross sections are for the production of singly charged ions only. Direct (short-dashed curve) = direct ionization, present paper; Total (solid curve) = direct ionization plus excitation-autoionization, present paper; Shul (circles) = experiment by Shul *et al.* [7]; Patton (triangles) = experiment by Patton *et al.* [8]; DM (dot-dashed curve) = theory, DM formalism Ref. [3]; Lotz (long-dashed curve) = theory, Lotz formula [2].

production of multiply charged ions. Some experiments detect the charge state of ions produced, while others simply measure the total ion current. The simple sum of the cross sections for the production of ions with different charge states is known as the counting ionization cross section, while the ion current measurement is known as the gross ionization cross section:

$$\sigma_{\text{count}} = \Sigma_q \sigma(q+), \tag{6}$$

$$\sigma_{\text{gross}} = \Sigma_q q \sigma(q+), \tag{7}$$

where $\sigma(q+)$ is the cross section for producing an ion with charge $q+$.

Since the BEB model calculates direct ionization cross sections for individual orbitals, we can estimate multiple ionization cross sections by assuming an inner-shell hole would

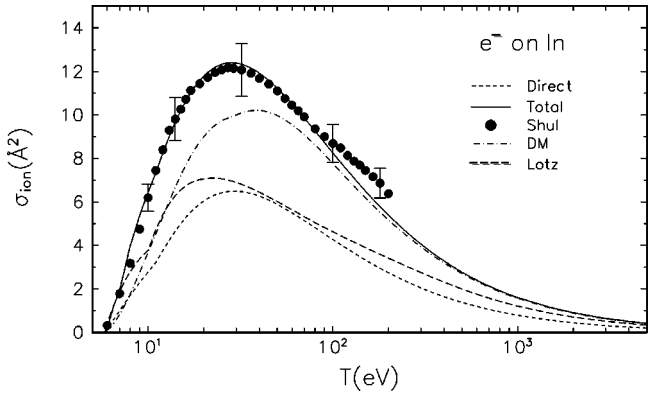

FIG. 4. Ionization cross section of In. All cross sections are for the production of singly charged ions only. Direct (short-dashed curve) = direct ionization, present paper; Total (solid curve) = direct ionization plus excitation-autoionization, present paper; Shul (circles) = experiment by Shul *et al.* Ref. [7]; DM (dot-dashed curve) = DM formalism Ref. [3]; Lotz (long-dashed curve) = Lotz formula [2].

TABLE I. Atomic parameters for the BEB and scaled Born calculations. U=orbital kinetic energy; B=binding energy; N=electron occupation number; E=excitation energy; $f_{sc}=f$ value from uncorrelated wave functions; $f_{mc}=f$ values calculated from MCDF wave functions. All values are theoretical except for the binding energies of the valence orbitals and the excitation energies of the autoionizing levels, which are experimental.

Orbital	B(eV)	U(eV)	N	Ground level	Excited level	E(eV)	f_{sc}	f_{mc}
				Boron				
$1s_{1/2}$	209.45	297.65	2	$2s^2 2p\ ^2P_{1/2}$	$2s2p^2\ ^2P_{1/2}$	8.992	0.605	0.402
$2s_{1/2}$	13.47	26.11	2		$2s2p^2\ ^2P_{3/2}$	8.993	0.334	0.203
$2p_{1/2}$	8.298	20.29	1					
				Aluminum				
$1s_{1/2}$	1595.50	2166.47	2	$3s^2 3p\ ^2P_{1/2}$	$3s3p^2\ ^2S_{1/2}$	6.417	0.138	0.0998
$2s_{1/2}$	134.13	297.91	2		$3s3p^2\ ^2P_{1/2}$	7.022	0.763	0.579
$2p_{1/2}$	87.85	269.64	2		$3s3p^2\ ^2P_{3/2}$	7.033	0.498	0.300
$2p_{3/2}$	87.37	267.96	4					
$3s_{1/2}$	10.73	25.59	2					
$3p_{1/2}$	5.986	15.56	1					
				Gallium				
$1s_{1/2}$	10 446.69	12 998.04	2	$4s^2 4p\ ^2P_{1/2}$	$4s4p^2\ ^2D_{3/2}$	6.67	0.636	0.457
$2s_{1/2}$	1341.54	2526.87	2		$4s4p^2\ ^2S_{1/2}$	7.700	0.182	0.147
$2p_{1/2}$	1182.02	2487.20	2		$4s4p^2\ ^2P_{1/2}$	8.159	0.726	0.567
$2p_{3/2}$	1154.00	2413.61	4		$4s4p^2\ ^2P_{3/2}$	8.236	0.495	0.313
$3s_{1/2}$	179.02	557.49	2					
$3p_{1/2}$	125.70	503.48	2					
$3p_{3/2}$	121.75	488.13	4					
$3d_{3/2}$	31.97	355.81	4					
$3d_{5/2}$	31.41	352.35	6					
$4s_{1/2}$	11.78	42.69	2					
$4p_{1/2}$	5.999	21.63	1					
				Indium				
$1s_{1/2}$	28 102.81	34 209.68	2	$5s^2 5p\ ^2P_{1/2}$	$5s5p^2\ ^2D_{3/2}$	6.121	0.746	0.545
$2s_{1/2}$	4297.46	7290.99	2		$5s5p^2\ ^2S_{1/2}$	7.055	0.326	0.289
$2p_{1/2}$	3995.30	7252.97	2		$5s5p^2\ ^2P_{1/2}$	7.397	0.679	0.491
$2p_{3/2}$	3783.43	6723.44	4		$5s5p^2\ ^2P_{3/2}$	7.520	0.496	0.306
$3s_{1/2}$	854.43	2083.45	2					
$3p_{1/2}$	731.28	2009.91	2					
$3p_{3/2}$	691.82	1889.58	4					
$3d_{3/2}$	476.43	1754.12	4					
$3d_{5/2}$	468.45	1722.46	6					
$4s_{5/2}$	144.30	516.24	2					
$4p_{1/2}$	102.02	454.83	2					
$4p_{3/2}$	94.99	426.00	4					
$4d_{3/2}$	27.96	284.85	4					
$4d_{5/2}$	26.96	277.94	6					
$5s_{5/2}$	10.70	50.93	2					
$5p_{1/2}$	5.786	26.10	1					

lead to a succession of Auger process resulting in the production of a multiply charged ion. For instance, we can assume a $2s$ or $2p$ hole in Al will eventually produce a doubly charged ion, and hence, we can double the L-shell ionization cross section to obtain σ_{gross}. In reality, some inner-shell vacancies may decay through fluorescence. The branching ratio between the decay by autoionization and by fluorescence is known as the fluorescence yield, and it is a major task to calculate reliable fluorescence yield. Doubling the L-shell ionization cross section as we have done for Al will give an upper limit.

The last columns in Tables II–V list σ_{count}. An upper limit to σ_{gross} is obtained by doubling or tripling cross sections of orbitals whose binding energies are high enough to

TABLE II. Cross sections for direct ionization, excitation to the $2s2p^2$ levels, and total counting ionization of B in Å^2 as functions of the incident electron energy T.

T(eV)	Direct, BEB counting	Excitation $^2P_{1/2}$	Excitation $^2P_{3/2}$	Total counting
9	0.094			0.094
10	0.233	0.415	0.217	0.865
12	0.491	0.665	0.347	1.503
15	0.904	0.848	0.441	2.193
20	1.564	0.984	0.509	3.058
25	1.991	1.034	0.534	3.558
30	2.257	1.046	0.539	3.842
40	2.519	1.022	0.525	4.066
50	2.596	0.975	0.500	4.071
60	2.587	0.923	0.473	3.984
70	2.538	0.874	0.448	3.859
80	2.470	0.827	0.424	3.721
90	2.394	0.785	0.402	3.581
100	2.315	0.747	0.382	3.444
125	2.125	0.665	0.340	3.130
150	1.956	0.600	0.306	2.862
175	1.809	0.547	0.279	2.635
200	1.681	0.503	0.257	2.441
225	1.571	0.466	0.238	2.276
250	1.475	0.435	0.222	2.132
275	1.391	0.408	0.208	2.007
300	1.316	0.384	0.196	1.896
400	1.086	0.313	0.160	1.559
500	0.928	0.266	0.135	1.329
600	0.812	0.232	0.118	1.162
700	0.723	0.206	0.105	1.034
800	0.653	0.186	0.095	0.934
900	0.596	0.169	0.086	0.852
1000	0.549	0.156	0.079	0.784

TABLE III. Cross sections for direct ionization, excitation to the $3s3p^2$ levels, and total counting ionization of Al in Å^2 as functions of the incident electron energy T.

T(eV)	Direct, BEB counting	Excitation $^2S_{1/2}$	Excitation $^2P_{1/2}$	Excitation $^2P_{3/2}$	Total counting
6	0.010				0.010
7	0.720	0.144			0.864
8	1.372	0.230	0.654	0.368	2.624
9	1.921	0.283	0.918	0.516	3.639
10	2.368	0.322	1.105	0.620	4.415
12	3.334	0.375	1.363	0.762	5.834
15	4.571	0.418	1.590	0.887	7.466
20	5.659	0.447	1.761	0.980	8.846
25	6.080	0.450	1.813	1.007	9.350
30	6.185	0.444	1.810	1.004	9.442
40	6.010	0.419	1.738	0.963	9.130
50	5.672	0.391	1.640	0.908	8.611
60	5.312	0.365	1.542	0.853	8.072
70	4.974	0.341	1.451	0.802	7.567
80	4.666	0.320	1.368	0.755	7.109
90	4.392	0.302	1.293	0.714	6.700
100	4.152	0.285	1.226	0.677	6.339
125	3.656	0.251	1.086	0.599	5.592
150	3.274	0.225	0.976	0.538	5.013
175	2.971	0.204	0.888	0.489	4.551
200	2.724	0.186	0.815	0.449	4.174
225	2.518	0.172	0.754	0.415	3.860
250	2.344	0.160	0.702	0.387	3.594
275	2.195	0.150	0.658	0.362	3.365
300	2.066	0.141	0.619	0.341	3.167
400	1.682	0.114	0.504	0.277	2.578
500	1.428	0.096	0.427	0.235	2.186
600	1.246	0.084	0.372	0.205	1.906
700	1.108	0.074	0.331	0.182	1.694
800	0.999	0.067	0.298	0.164	1.528
900	0.912	0.061	0.272	0.149	1.394
1000	0.840	0.056	0.250	0.137	1.283

trigger Auger processes that produce doubly or triply charged ions. For example, a $3p$ hole in Ga should provide enough energy (see Table I) to produce a triply charged ion through successive Auger transitions. The $3p$ hole can also produce doubly charged ions, or decay by fluorescence. Detailed analysis of branching ratios of these competing processes is beyond the scope of the present paper.

With the same kind of reasoning, we can determine ionization cross sections for producing a singly charged ion by adding cross sections only from orbitals whose binding energies are low enough not to produce multiply charged ions through Auger transitions into the inner-shell holes created. The total ionization cross sections shown as solid curves in Figs. 1–4 are for the production of singly charged ions only. Such cross sections are calculated by summing cross sections only from the outer orbitals with the highest principal quantum numbers.

A rigorous treatment of the excitation-autoionization contributions would have mixed the amplitude of the underlying direct ionization channel with the amplitudes of the excitation-autoionization channels. This type of mixing could lead to constructive or destructive interference between the two amplitudes, thus producing resonances. A simple sum of the direct ionization and autoionization cross sections as we have done amounts to assuming fully constructive interference resulting in no resonances.

The DM formalism by Margreiter *et al.* [3] is a semiempirical expression with constants determined by fitting to experimental data for ionization of a large number of atoms. The DM formalism does not distinguish excitation-autoionization from direct ionization, and therefore, cannot effectively describe cross sections when autoionization is large. As expected, the Lotz cross sections are close to the direct ionization cross sections, but fails to account for the contributions from excitation-autoionization.

Freund *et al.* [1] prepared target atoms by neutralizing ions by charge transfer, which often produced neutral atoms both in their ground state as well as in metastable states that have the same electron configuration as the ground state. For

TABLE IV. Cross sections for direct ionization, excitation to the $4s4p^2$ levels, and total counting ionization of Ga in Å^2 as functions of the incident electron energy T.

T(eV)	Direct, BEB counting	Excitation $^2D_{3/2}$	Excitation $^2S_{1/2}$	Excitation $^2P_{1/2}$	Excitation $^2P_{3/2}$	Total counting
6.5	0.360					0.360
7	0.720	0.453				1.173
8	1.382	0.879	0.091			2.352
9	1.938	1.125	0.186	0.439	0.230	3.917
10	2.389	1.300	0.242	0.647	0.349	4.927
12	3.079	1.535	0.315	0.914	0.497	6.341
15	4.182	1.735	0.379	1.153	0.629	8.078
20	5.190	1.873	0.429	1.353	0.740	9.585
25	5.598	1.901	0.447	1.436	0.786	10.167
30	5.712	1.881	0.450	1.462	0.800	10.304
40	5.757	1.787	0.436	1.440	0.789	10.209
50	5.654	1.675	0.414	1.381	0.756	9.881
60	5.480	1.568	0.391	1.312	0.719	9.471
70	5.285	1.470	0.369	1.245	0.682	9.051
80	5.087	1.382	0.349	1.181	0.647	8.647
90	4.897	1.304	0.331	1.123	0.615	8.270
100	4.717	1.234	0.314	1.069	0.586	7.920
125	4.315	1.089	0.279	0.955	0.523	7.162
150	3.987	0.976	0.252	0.863	0.473	6.551
175	3.710	0.886	0.229	0.789	0.432	6.046
200	3.473	0.812	0.211	0.727	0.398	5.621
225	3.268	0.751	0.195	0.674	0.370	5.258
250	3.088	0.698	0.182	0.630	0.345	4.943
275	2.929	0.653	0.171	0.591	0.324	4.668
300	2.788	0.614	0.161	0.557	0.305	4.425
400	2.345	0.499	0.131	0.456	0.250	3.679
500	2.032	0.422	0.111	0.388	0.212	3.165
600	1.798	0.367	0.097	0.338	0.185	2.786
700	1.616	0.326	0.086	0.301	0.165	2.494
800	1.470	0.293	0.078	0.272	0.149	2.261
900	1.350	0.267	0.071	0.248	0.136	2.072
1000	1.249	0.245	0.065	0.229	0.125	1.913

the Group IIIB atoms, some fraction of the target atoms must have been in the $ns^2np\ ^2P_{3/2}$ level instead of the $^2P_{1/2}$ level. The energy resolution of the incident electron beam used by Freund *et al.* was 0.7 eV at full width half maximum, which is more than twice the fine-structure splitting in the ground state of indium. The sum of the direct and indirect ionization cross sections for light atoms are not expected to be affected by the fine structure because the two levels are very close. For heavier members, however, small difference may develop because the fine-structure splitting is discernible—0.27 eV for In, for instance—and a new autoionizing level, $nsnp^2\ ^2D_{5/2}$, can be reached by dipole interaction from the $^2P_{3/2}$ metastable level, but not from the $^2P_{1/2}$ ground level. We calculated both direct and indirect ionization cross sections from the metastable level, and found practically no difference for boron as expected. The peak values of the ionization cross sections from the metastable levels of other atoms were slightly higher than those from the ground levels, reaching a maximum difference of approximately 4% for indium. Hence, we conclude that the presence of metastable target atoms would not have seriously affected experimental data for the Group IIIB atoms by Freund *et al.* [1]. This is not true of other atoms such as phosphorus according to Freund *et al.* [1].

A. Boron

For boron, only the $2s2p^2\ ^2P_{1/2}$ and $^2P_{3/2}$ levels are above the first ionization threshold, and the solid curve in Fig. 1 is the sum of the direct ionization (includes all bound electrons) represented by the short-dashed curve and autoionization from these excited states. To obtain accurate f values for the f scaling of the $2s^22p\ ^2P_{1/2}$–$2s2p^2\ ^2P_{1/2}$, and $^2P_{3/2}$ excitation cross sections (Table I), we used multiconfiguration Dirac-Fock (MCDF) wave functions equivalent to the nonrelativistic configurations $2s^22p+2p^3+2p3d^2+3d^3$ for the ground state and $2s2p^2+2p^23d+2s3d^2+2s2p3d$ for the excited states. The f_{mc} values for boron

TABLE V. Cross sections for direct ionization, excitation to the $5s5p^2$ levels, and total counting ionization of In in Å^2 as functions of the incident electron energy T.

T(eV)	Direct, BEB counting	Excitation $^2D_{3/2}$	Excitation $^2S_{1/2}$	Excitation $^2P_{1/2}$	Excitation $^2P_{3/2}$	Total counting
6	0.173					0.173
7	0.988	0.953				1.941
8	1.707	1.361	0.350	0.367	0.194	3.979
9	2.297	1.639	0.497	0.607	0.346	5.386
10	2.769	1.846	0.602	0.773	0.450	6.440
12	3.763	2.132	0.746	1.008	0.595	8.243
15	4.993	2.374	0.875	1.223	0.728	10.193
20	6.041	2.533	0.973	1.399	0.839	11.785
25	6.421	2.553	1.004	1.466	0.882	12.326
30	6.607	2.514	1.004	1.480	0.892	12.497
40	6.797	2.373	0.966	1.442	0.872	12.450
50	6.731	2.215	0.912	1.373	0.831	12.063
60	6.557	2.067	0.858	1.299	0.787	11.568
70	6.342	1.933	0.808	1.228	0.745	11.055
80	6.115	1.814	0.762	1.162	0.705	10.559
90	5.891	1.709	0.721	1.102	0.669	10.092
100	5.679	1.616	0.684	1.047	0.636	9.662
125	5.213	1.423	0.606	0.932	0.567	8.740
150	4.815	1.273	0.545	0.840	0.511	7.985
175	4.476	1.154	0.496	0.766	0.466	7.358
200	4.183	1.057	0.455	0.705	0.429	6.830
225	3.929	0.976	0.421	0.654	0.398	6.378
250	3.705	0.908	0.392	0.610	0.371	5.987
275	3.507	0.849	0.368	0.572	0.348	5.644
300	3.331	0.798	0.346	0.539	0.328	5.342
400	2.782	0.647	0.282	0.440	0.268	4.419
500	2.398	0.547	0.239	0.374	0.228	3.785
600	2.114	0.476	0.208	0.326	0.199	3.323
700	1.895	0.422	0.185	0.290	0.177	2.968
800	1.720	0.380	0.167	0.262	0.160	2.687
900	1.576	0.346	0.152	0.239	0.146	2.459
1000	1.457	0.318	0.140	0.220	0.134	2.269

listed in Table I are about 4% larger than the values adapted by Verner *et al.* [33] from the Opacity Project data. We used our own f_{mc} values to be consistent with the autoionization rates we calculated to determine the branching ratios for fluorescent decay of the autoionizing levels. Using the f values from the Opacity Project (0.390 and 0.195 for the excitations to the $^2P_{1/2}$ and $^2P_{3/2}$ levels, respectively) would have reduced the peak value of the solid curve in Fig. 1 by a few percent. The branching ratios for autoionization calculated from these MCDF wave functions are 99.8% for the $^2P_{1/2}$ autoionizing level and 99.5% for the $^2P_{3/2}$ autoionizing level.

In addition to the Lotz and DM cross sections, Fig. 1 also includes the total ionization cross section recommended by Moores [34], who scaled the cross sections for isoelectronic ions. All theoretical data presented in Fig. 1 include direct ionization of all target electrons. Earlier, Stingl [35] reported Coulomb-Born cross sections that included exchange effect between the incident and target electrons for B, C^+, N^{++}, and O^{3+}. The Stingl data (circles) in Fig. 1 include the direct ionization of both the $2p$ and $2s$ electrons but not the excitation-autoionization of the $2s$ electrons. For neutral boron, Stingl used plane waves instead of Coulomb waves. Her results are clearly too high compared to our data and those by Moores for direct ionization, both of which include contributions from the $2p$ and $2s$ electrons.

B. Aluminum

The autoionizing levels that we have included for Al are the $3s3p^2\,^2S_{1/2}$, $^2P_{1/2}$, and $^2P_{3/2}$ levels. The $3s3p^2\,^2P_{1/2,3/2}$ levels of Al are known to autoionize much faster than to decay by fluorescence [36] even though different parities reduce the autoionization rate, as was mentioned earlier. As can be seen from Table III, the two autoionizing $^2P_{1/2,3/2}$ levels contribute four to seven times as much to the total ionization cross section as the autoionizing $^2S_{1/2}$ level. As was mentioned earlier, the $3s3p^2\,^2D_{3/2,5/2}$ levels are not

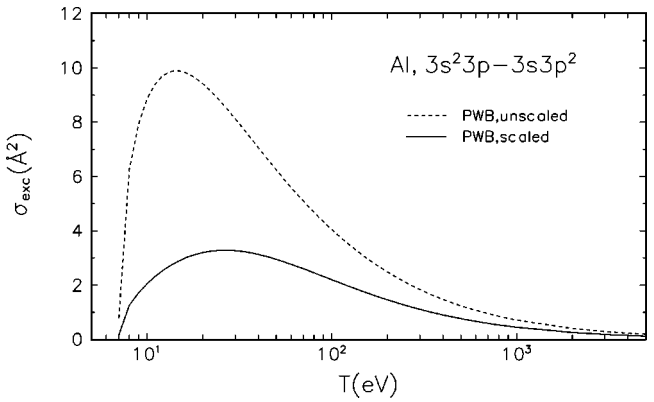

FIG. 5. Comparison of unscaled and scaled plane-wave Born cross sections for Al. PWB, unscaled (dashed curve) = sum of unscaled PWB cross sections for autoionizing excitations; PWB, scaled (solid curve) = sum of scaled PWB cross sections for autoionizing excitations. Branching ratios for autoionization and fluorescence have also been applied to the scaled Born cross sections.

observed above the ionization limit in Al, but are instead mixed with the $3s^2nd$ bound states of the neutral atom [19].

The effect of fluorescent decay was estimated using the branching ratios calculated from the autoionizing and fluorescent decay rates with the MCDF wave functions mentioned below. The branching ratios so obtained for ionization from the $3s3p^2\,^2P_J$ levels are 0.882 for $J=1/2$ and 0.933 for $J=3/2$. The autoionization branching ratio for the $^2S_{1/2}$ level calculated from the MCDF wave functions is very close to unity. The order of magnitude of our fluorescent decay rates are in agreement with those used by Lombardi *et al.* [36] to deduce experimental autoionization rates from observed line widths of the $3s3p^2\,^2P$ levels. Our theoretical autoionization rates are 1.4×10^{10} sec^{-1} and 2.6×10^{10} sec^{-1} for the $^2P_{1/2}$ and the $^2P_{3/2}$ levels, respectively, while the corresponding values reported by Lombardi *et al.* are $4.0\pm0.4\times10^{10}$ sec^{-1} and $0.87\pm0.11\times10^{10}$ sec^{-1}. We used our theoretical values to be consistent with the rest of our cross sections.

The f_{mc} values for the f scaling of the $3s^23p\,^2P_{1/2}$–$3s3p^2\,^2S_{1/2}$, $^2P_{1/2}$, and $^2P_{3/2}$ excitation cross sections (Table I) were calculated from MCDF wave functions equivalent to the nonrelativistic configurations $3s^23p+3p^3+3p3d^2+3s3p3d$ for the ground state and $3s3p^2+3p^23d+3s3d^2+3d^3$ for the excited states. The f values adapted by Verner *et al.* [33] from the Opacity Project data are about 7 to 17 % lower than the f_{mc} values in Table I. Using the f values from the Opacity Project (0.531 and 0.266 for the excitations to the $^2P_{1/2}$ and $^2P_{3/2}$ levels, respectively) would have reduced the peak value of the solid curve in Fig. 2 by about 3%. The sum of these excitation-autoionization cross sections, both scaled and unscaled, are compared in Fig. 5, to demonstrate dramatic reduction of the unscaled PWB cross sections through the BE and f scaling. Reductions of this magnitude were also common in resonance transitions of alkali metals and alkaline-earth elements [11]. This undoubtedly contributed to the sizable overestimate by McGuire [5], which was based on unscaled PWB approximation.

Plane-wave Born cross sections for excitations to 10 levels from the $3s3p3d$ configuration and 13 levels from the $3s3p4p$ configuration were calculated with configuration-averaged Dirac-Fock wave functions to estimate the magnitude of their contributions to autoionization. Scaling was not applied to the PWB cross sections for the $3s3p3d$ excitations because they are dipole-forbidden excitations, and it is known that PWB cross sections underestimate such cross sections [37] by as much as a factor of two. In this case, scaling would introduce more errors. The BE- and f-scaled PWB cross sections were used for the dipole-allowed excitations to the $3s3p4p$ levels. The total contribution from the $3s3p3d$ and $3s3p4p$ excitations calculated in this way amounted to 4% for the former at the cross-section peak and less than 1% for the latter. The solid curve in Fig. 2 include these additional contributions. The ''bulge'' in the experimental data in Fig. 2 between $T=10$ and 20 eV is most likely from the autoionization of higher-excited levels we have not accounted for, and to some extent, the failure of the unscaled PWB cross sections we have used for the $3s3p3d$ excitations.

The curve marked ''Total, gross'' in Fig. 2 (visible at $T>200$ eV) represents our estimate of the gross ionization cross section, indicating that the production of multiply charged ions is not significant for Al.

C. Gallium

For Ga, all doublet levels from the $4s4p^2$ configuration, $^2D_{3/2}$, $^2D_{5/2}$, $^2S_{1/2}$, $^2P_{1/2}$, and $^2P_{3/2}$ levels, are above the first ionization threshold. However, the $^2D_{5/2}$ excited level cannot be reached from the ground level $4s^24p\,^2P_{1/2}$ by a dipole-allowed excitation. Instead, it is a magnetic-quadrupole transition because it requires $\Delta J=2$ and parity change. Accordingly, electron-impact excitation cross section to the $^2D_{5/2}$ level is extremely small, and we excluded it from our calculation. As was mentioned earlier, however, the $^2D_{5/2}$ level can be reached by a dipole-allowed excitation from the metastable ground level, $4s^24p\,^2P_{3/2}$. This transition is strong as expected, but the excitation to the $^2D_{3/2}$ level decreases sharply, making the sum of the two cross sections comparable to the excitation from the ground state to the $^2D_{3/2}$ level. According to Patton *et al.* [8], their target atoms were all in the normal ground level. Since the target atoms in the experiment by Shul *et al.* [7] were produced by charge transfer to Ga^+, their target atom beam must have contained some metastable Ga atoms. The experimental cross section, however, is unlikely to have been affected by the presence of metastable targets as was explained earlier. Accurate f values used for the f scaling (Table I) were calculated from MCDF wave functions similar to those used for Al. The autoionization branching ratios calculated from these MCDF wave functions all exceeded 99%.

The detailed experimental data for Ga by Patton *et al.* [8] show a structure just above the threshold at about 7.5, 10, and 14 eV. Similar structure is present in the data by Shul *et al.* [7] though it is not as pronounced. These energies correspond to the threshold for excitation to autoionizing levels of Ga. In particular, the first set of autoionizing levels are at

6.67, 7.70, and 8.2 eV above the ground level, overlapping the first element of structure in the Patton data. These are precisely the autoionizing levels that have been included in our calculations. We do not observe, however, the structure clearly visible in the data by Patton *et al.*, though our cross sections are increased significantly at higher energies by the presence of these levels. This is consistent with excitation cross sections for the dipole-allowed transitions reaching their peak values at energies that are much higher than the threshold energy and not contributing significantly at threshold.

Excitations to the $4s4pnp$ levels of Ga for $n \geqslant 5$ are small because of the higher principal quantum numbers. Our calculation for excitations to the $4s4p5p$ levels is only 0.6% of the cross sections for the excitation to the $4s4p^2$ levels at the peak. Excitations to the $4s4p4d$ levels are also small (2.3% at the peak) because these levels are dipole-forbidden transitions as in the case of Al. We did not include these excitations to higher levels in the solid curve shown in Fig. 3 because we estimate that altogether they will contribute about 4% or less at the peak. In spite of these simplifications, our total ionization cross section in Fig. 3 agrees better with the experimental data by Patton *et al.* [8] than those by Shul *et al.* [7] at all T.

D. Indium

As is the case for Ga, all doublet levels, $^2D_{3/2}$, $^2D_{5/2}$, $^2S_{1/2}$, $^2P_{1/2}$, and $^2P_{3/2}$ from the $5s5p^2$ configuration are autoionizing [38]. Excitation to the $^2D_{5/2}$ level was omitted because it was very small as was explained for Ga. Again, Fig. 4 demonstrates that the DM and Lotz cross sections are too low, while our total ionization cross section agrees well with the experiment by Shul *et al.* [7]. The shape of the data by Shul *et al.* [7] for both Ga and In at $T > 100$ eV in Figs. 3 and 4 suggests some experimental difficulties. This discrepancy in the cross section shape at $T > 100$ eV between the BEB cross sections and those measured by the Bell Laboratories group (e.g., Freund *et al.* [1]) is observed in many targets, including some molecules [16]. All autoionization branching ratios calculated from MCDF wave functions similar to those used for Al are practically unity.

E. Autoionization in Other Atoms

As the preceding examples have indicated, a core-excited level contributes significantly to autoionization when all of the following conditions are met in addition to the obvious requirement that the excited level should lie above the first ionization limit:

(a) the core electron being excited should have the same principal quantum number as the valence electron, and the excited levels of the core electron should also have the same principal quantum number;

(b) the excitation should be spin and dipole allowed; and

(c) the branching ratio of the excited level between autoionization and fluorescent decay should be strongly in favor of the former.

For example, these conditions are met by the $2s2p^3\,^3S$ level of carbon, because the ground level is also a triplet, $2s^22p^2\,^3P$. Other $2s2p^3$ levels above the first ionization limit are singlets, thus violating condition (b). Our preliminary results on carbon indicate that about 14% of the peak ionization cross section comes from the autoionization of the ^3S level.

In contrast, atoms in the Group VB headed by nitrogen are not subject to strong excitation-autoionization because the ground level, ns^2np^3 is ^4S, while the only quartet level from the $nsnp^4$ configuration is ^4P, which lies below the first ionization limit. On the other hand, ionization of metastable atoms in this group will be increased by excitation-autoionization to $nsnp^4$ doublet levels.

Oxygen will have a discernible autoionization contribution from the $2s2p^5\,^3P$ level, which has the same spin as the ground level, $2s^22p^4\,^3P$. Similarly, fluorine is expected to have an autoionization contribution from the $2s2p^6\,^2S$ level. The fact that an atom that heads a column in the periodic table has strong autoionization is not a guarantee that heavier atoms in the same column would also have strong autoionization. For example, the $3s3p^5\,^3P$ level of sulfur and the $4s4p^6\,^2S$ level of bromine lie below the first ionization limit, indicating the need to examine each atom carefully, including condition (c) and the possibility of the excited state losing its identity through strong mixing with a Rydberg series in the discrete spectrum, as was the case for the $3s3p^2\,^2D$ level of aluminum.

Heavier alkali metals (K, Rb, Cs, Fr) and alkaline-earth elements (Ca, Sr, Ba, and Ra) are also likely candidates because excitations of the core np electrons to the nd states should contribute significantly to autoionization, as was shown for Rb [39]. The theoretical total ionization cross section of Rb in Ref. [39] may be improved by applying the BE and f scalings of PWB cross sections used in this article.

IV. CONCLUSIONS

It is clear that autoionization contributes about as much to the total ionization of boron, aluminum, gallium, and indium as does direct ionization. It is also clear that the first set of autoionizing levels ($nsnp^2$) accounts for nearly all the autoionization (where $n=2$ for B, $n=3$ for Al, $n=4$ for Ga, and $n=5$ for In). Accurate results are obtained using the BEB cross sections for direct ionization and scaled Born cross sections for excitations to the autoionizing levels.

Although indirect ionization processes such as excitation-autoionization are a common occurrence, it is unusual in neutral atoms to have the indirect process contribute almost as much as the direct ionization cross section. As was explained earlier, excitation-autoionization may have significant contributions to the total ionization cross sections whenever all conditions listed in Sec. III E are met. Some of the atoms that satisfy such conditions but not included in the present paper are C, O, F, heavy alkali metals, heavy alkaline-earth elements, and Tl.

The comparisons with available experimental data are clear examples of the validity of the BE and f scaling of PWB cross sections. The unscaled Born cross sections need not be produced from highly correlated wave functions. As long as accurate matching f values are available, Born cross

sections from uncorrelated Hartree-Fock or Dirac-Fock wave functions should be sufficient.

Cross sections for ionizing Group IIIB atoms in the metastable $ns^2np\,^2P_{3/2}$ level are only slightly higher than the cross sections from the ground level. Hence, the experimental data by Freund *et al.* [1] and by Shul *et al.* [7] would not have been affected by the amount of metastable atoms in their target beams.

The present combination of the BEB model for direct ionization and scaled Born cross sections for excitation autoionization can generate electron-impact ionization cross sections of modest accuracy ($\pm 15\%$ or better at the peak) with reliable overall dependence on the incident energy for a wide range of neutral, open-shell atoms. The present method provides ionization cross sections suitable for many applications, such as modeling of fusion plasmas, semiconductor fabrication, astrophysics, and mass spectrometric study of materials including high-temperature mass spectrometry, while using orders of magnitude less computing resources than other theories that can assure comparable accuracy. At present, however, most such theories are not mature enough to handle heavy atoms such as In, for which relativistic wave functions are desirable to distinguish the fine structure in the target.

ACKNOWLEDGMENTS

This work was supported in part by the Office of Fusion Energy Sciences, U.S. Department of Energy, and the Advanced Technology Program, NIST. We thank Dr. John Hastie of NIST for calling our attention to the unusually high ionization cross sections of Al. We are grateful to Dr. J. P. Desclaux and Dr. P. Indelicato for providing us with the latest version of the Dirac-Fock wave function code. P.M.S. would like to thank the Physics Laboratory at the National Institute of Standards and Technology for its hospitality as a guest scientist.

[1] R. S. Freund, R. C. Wetzel, R. J. Shul, and T. R. Hayes, Phys. Rev. A **41**, 3575 (1990).
[2] W. Lotz, Z. Phys. **232**, 101 (1970); **60**, 206 (1970).
[3] D. Margreiter, H. Deutsch, and T. Märk, Int. J. Mass Spectrom. Ion Processes **139**, 127 (1994).
[4] M. Gryzinski, Phys. Rev. **138**, A305 (1965); **138**, A322 (1965); **138**, A336 (1965).
[5] E. J. McGuire, Phys. Rev. A **26**, 125 (1982).
[6] J. B. Mann, J. Chem. Phys. **46**, 1646 (1967).
[7] R. J. Shul, R. C. Wetzel, and R. S. Freund, Phys. Rev. A **39**, 5588 (1989).
[8] C. J. Patton, K. O. Lozhkin, M. B. Shah, J. Geddes, and H. B. Gilbody, J. Phys. B **29**, 1409 (1996).
[9] G. Peach, J. Phys. B **3**, 329 (1970).
[10] Y.-K. Kim and M. E. Rudd, Phys. Rev. A **50**, 3954 (1994).
[11] Y.-K. Kim, Phys. Rev. A **64**, 032713 (2001).
[12] P. Burke and K. Berrington, *Atomic and Molecular Processes: An R-Matrix Approach* (Institute of Physics Publishing, Bristol, 1993).
[13] I. Bray and A. T. Stelbovics, Adv. At., Mol., Opt. Phys. **35**, 209 (1995).
[14] F. Robicheaux, M. S. Pindzola, and D. R. Plante, Phys. Rev. A **55**, 3573 (1997).
[15] M. Baertschy, T. N. Rescigno, W. A. Isaacs, X. Li, and C. W. McCurdy, Phys. Rev. A **63**, 022712 (2001).
[16] See NIST's public website http://physics.nist.gov/ionxsec
[17] Y.-K. Kim, W. R. Johnson, and M. E. Rudd, Phys. Rev. A **61**, 034702 (2000).
[18] Y.-K. Kim, J. P. Santos, and F. Parente, Phys. Rev. A **62**, 052710 (2000).
[19] A. W. Weiss, Phys. Rev. A **9**, 1524 (1974).
[20] N. F. Mott, Proc. R. Soc. London, Ser. A **126**, 259 (1930).
[21] L. Vriens, in *Case Studies in Atomic Physics*, edited by E. W. McDaniel and M. R. C. McDowell (North Holland, Amsterdam, 1969), Vol. 1, p. 335.
[22] H. Bethe, Ann. Phys. (Leipzig) **5**, 325 (1930).
[23] M. Inokuti, Rev. Mod. Phys. **43**, 297 (1971).
[24] H. A. Bethe and E. E. Salpeter, *Quantum Mechanics of One- and Two-Electron Atoms* (Springer-Verlag, Berlin, 1957), p. 304.
[25] J. P. Desclaux, in *Methods and Techniques in Computational Chemistry: METECC-94, Vol. A: Small Systems*, edited by E. Clementi (STEF, Cagliari, 1993), Chap. 5.
[26] W. Hwang, Y.-K. Kim, and M. E. Rudd, J. Chem. Phys. **104**, 2956 (1996).
[27] A. Burgess, *Proceedings of the Third International Conference on Electronic and Atomic Collisions, London, 1963*, edited by M. R. C. McDowell (North Holland, Amsterdam, 1964), p. 237.
[28] S. M. Younger and W. L. Wiese, J. Quant. Spectrosc. Radiat. Transf. **22**, 161 (1979).
[29] See, for example, NIST's public website: http://physics.nist.gov
[30] L. L. Shimon, É. I. Nepiipov, and I. P. Zapesochnyi, Zh. Tekh. Fiz. **45**, 688 (1975) [Sov. Phys. Tech. Phys. **20**, 434 (1975)].
[31] D. G. Golovach, A. N. Drozdov, V. I. Rakhovskii, and V. M. Shustryakov, Meas. Tech. **30**, 587 (1987).
[32] L. A. Vainshtein, D. G. Golovach, V. I. Ochkur, V. I. Rakhovskii, N. M. Rumyantsev, and V. M. Schustryakov, Zh. Eksp. Teor. Fiz. **93**, 65 (1987) [Sov. Phys. JETP **66**, 36 (1987)].
[33] D. A. Verner, E. M. Verner, and G. J. Ferland, At. Data Nucl. Data Tables **64**, 1 (1996).
[34] D. L. Moores, Phys. Scr., T **62**, 19 (1996).
[35] E. Stingl, J. Phys. B **5**, 1160 (1972).
[36] G. G. Lombardi, B. L. Cardon, and R. L. Kurucz, Astrophys. J. **248**, 1202 (1981).
[37] A. H. Mahan, A. Gallagher, and S. J. Smith, Phys. Rev. A **13**, 156 (1976).
[38] W. R. S. Garton, W. H. Parkinson, and E. M. Reeves, Can. J. Phys. **44**, 1745 (1966).
[39] Y.-K. Kim, J. Migdalek, W. Siegel, and J. Bieroń, Phys. Rev. A **57**, 246 (1998).